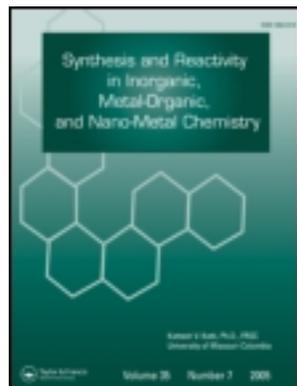


This article was downloaded by: [National Pingtung University of Science and Technology]

On: 22 October 2013, At: 08:26

Publisher: Taylor & Francis

Informa Ltd Registered in England and Wales Registered Number: 1072954 Registered office: Mortimer House, 37-41 Mortimer Street, London W1T 3JH, UK



## Synthesis and Reactivity in Inorganic, Metal-Organic, and Nano-Metal Chemistry

Publication details, including instructions for authors and subscription information:

<http://www.tandfonline.com/loi/lsrt20>

### Nanocomposite Catalysts Obtaining by Mechanochemical Technique for Synthesizing Carbon Nanotubes

E. Z. Karimi<sup>a</sup>, J. Vahdati-Khaki<sup>a</sup>, S. M. Zebarjad<sup>a</sup>, I. A. Bataev<sup>b</sup> & A. G. Bannov<sup>c</sup>

<sup>a</sup> Department of Materials and Metallurgical Engineering, Faculty of Engineering, Ferdowsi University of Mashhad, Mashhad, I. R. Iran

<sup>b</sup> Department of Mechanical Engineering, Novosibirsk State Technical University, Novosibirsk, Russia

<sup>c</sup> Department of Chemical Engineering, Novosibirsk State Technical University, Novosibirsk, Russia

Accepted author version posted online: 05 Sep 2013. Published online: 21 Oct 2013.

To cite this article: E. Z. Karimi, J. Vahdati-Khaki, S. M. Zebarjad, I. A. Bataev & A. G. Bannov (2014) Nanocomposite Catalysts Obtaining by Mechanochemical Technique for Synthesizing Carbon Nanotubes, *Synthesis and Reactivity in Inorganic, Metal-Organic, and Nano-Metal Chemistry*, 44:2, 212-221, DOI: [10.1080/15533174.2013.769590](https://doi.org/10.1080/15533174.2013.769590)

To link to this article: <http://dx.doi.org/10.1080/15533174.2013.769590>

PLEASE SCROLL DOWN FOR ARTICLE

Taylor & Francis makes every effort to ensure the accuracy of all the information (the "Content") contained in the publications on our platform. However, Taylor & Francis, our agents, and our licensors make no representations or warranties whatsoever as to the accuracy, completeness, or suitability for any purpose of the Content. Any opinions and views expressed in this publication are the opinions and views of the authors, and are not the views of or endorsed by Taylor & Francis. The accuracy of the Content should not be relied upon and should be independently verified with primary sources of information. Taylor and Francis shall not be liable for any losses, actions, claims, proceedings, demands, costs, expenses, damages, and other liabilities whatsoever or howsoever caused arising directly or indirectly in connection with, in relation to or arising out of the use of the Content.

This article may be used for research, teaching, and private study purposes. Any substantial or systematic reproduction, redistribution, reselling, loan, sub-licensing, systematic supply, or distribution in any form to anyone is expressly forbidden. Terms & Conditions of access and use can be found at <http://www.tandfonline.com/page/terms-and-conditions>

# Nanocomposite Catalysts Obtaining by Mechanochemical Technique for Synthesizing Carbon Nanotubes

E. Z. Karimi,<sup>1</sup> J. Vahdati-Khaki,<sup>1</sup> S. M. Zebarjad,<sup>1</sup> I. A. Bataev,<sup>2</sup>  
and A. G. Bannov<sup>3</sup>

<sup>1</sup>Department of Materials and Metallurgical Engineering, Faculty of Engineering, Ferdowsi University of Mashhad, Mashhad, I. R. Iran

<sup>2</sup>Department of Mechanical Engineering, Novosibirsk State Technical University, Novosibirsk, Russia

<sup>3</sup>Department of Chemical Engineering, Novosibirsk State Technical University, Novosibirsk, Russia

In the current research reactive milling was employed to fabricate the nanocomposite precursors for the catalytic growth of carbon nanostructures. For this purpose several mixtures of iron oxide and aluminum powders along with different amounts of graphite powders were mechanically milled for different times. The adiabatic temperature and the heat released from exothermic reaction during milling were controlled by varying the percentage of graphite. Synthesized powders were analyzed by X-ray diffraction, scanning electron microscope, transmission electron microscope, and thermogravimetric analysis. Propane gas was used in a chemical vapor deposition technique as a source of carbon to synthesize carbon nanotubes (CNTs). The results show that decomposition efficiency of propane promotes in the case of using milled powders and leads to a high yield of CNTs formation. The mechanical induced reaction between aluminum and iron oxide in the presence of graphite was used to produce micron-sized composite particles. These particles contain separated iron nanoparticles and dispersed in the matrix of ball milled graphite and alumina. It was found that the yield of fabrication of CNTs increased as decomposition temperature of propane increased from 625 to 850°C. Microscopic evaluation by SEM proved that the productivity of CNTs grown on milling derived catalysts was much high at higher annealing temperatures (700°C and 850°C) rather than that of lower temperature (625°C). The results of TGA tests showed that the amount of produced carbon nanotube depends on annealing temperature and as annealing temperature changed from 652 to 850°C carbon nanotube content increased from 13 to 85 wt%. TEM results demonstrated that CNTs were grown according to tip-growth mechanism.

**Keywords** carbon nanotube, mechanochemical process, nanocomposite, reactive milling

Received 8 December 2012; accepted 19 January 2013.

Address correspondence to E. Z. Karimi, Department of Materials and Metallurgical Engineering, Faculty of Engineering, Ferdowsi University of Mashhad, Mashhad, I. R. Iran. E-mail: ebrahimzk88@gmail.com

## INTRODUCTION

During the last two decades carbon nanomaterials such as fullerenes, carbon nanotubes (CNTs), and graphene have been under attention by researchers. Achieving the growth of high-quality CNTs at a low cost and on a large scale has been a problem in the past 20 years. The problem has been explored by many research groups, which have looked at fundamental science, engineering science, scale-up technology, and commercialization.<sup>[1]</sup> Nowadays, chemical vapor deposition (CVD) is the most-promising method for CNT mass production due to its much higher yield and simpler equipment, with respect to arc discharge and laser ablation methods.<sup>[2,3]</sup>

To obtain high-quality CNTs by CVD method, one of the key processes is to produce sufficiently small metallic particles, as catalysts, which are active enough for the formation of CNTs.<sup>[4,5]</sup> Indeed, the morphology of the obtained catalytic nanoparticles depends strongly on their fabrication method.<sup>[4]</sup> These nanoparticles can be produced by different methods, such as sol-gel,<sup>[6]</sup> coprecipitation,<sup>[7]</sup> ion-exchange-precipitation,<sup>[8,9]</sup> vapor or sputter deposition of a thin metallic layer on the substrate,<sup>[10]</sup> and impregnation processes,<sup>[11]</sup> as well as the formation of the solid solution between the parent oxides.<sup>[12]</sup>

Aggregation particles of catalysts upon drying is a big problem in impregnation and deposition from solution techniques.<sup>[13]</sup> The precursors obtained by these methods are generally required to be thermally treated at certain temperature in order to get desirable phase compositions, for instance, the decomposition of nitrates into oxides.<sup>[12]</sup> This causes the formation of large-sized agglomerations and to entrap a large amount of catalyst precursors inside them, which leads definitely to decrease the yield of formation of CNTs.<sup>[12,14]</sup> As a solution method, ball milling in general and mechanochemical processing in particular are powerful tools for producing nano-sized powders and nanocomposite materials,<sup>[14–16]</sup> and also can be used for obtaining homogeneous distribution of nano-sized particles into a solid matrix.<sup>[17,18]</sup>

With the pioneering work done by Ding et al.,<sup>[19]</sup> the mechanochemical process has been recognized as a unique technique for synthesizing Fe nanoparticles (which is well-known catalyst for CNTs synthesis)<sup>[20]</sup> and Fe-based nanocomposite materials.<sup>[19,21]</sup> One of the big significances of mechanochemical process is the formation of separated nanoparticles embedded into a solid matrix. By selecting suitable conditions such as chemical reaction paths, stoichiometry of starting materials and milling conditions, mechanochemical process can be used to synthesize nanocrystalline particles dispersed within a solid matrix,<sup>[22]</sup> which can be used as catalyst for CNT synthesis. For instance, Ding et al.<sup>[12]</sup> employed mechanochemical process for the preparation of  $\text{Al}_2\text{O}_3/\text{M}$  ( $\text{M} = \text{Fe}, \text{Co}, \text{Ni}$ ) nanocomposites and in which MWCNTs and SWCNTs were grown with high yields. Xiaomei et al.<sup>[23]</sup> applied continuous ball-milling of the yttria, aluminum hydroxide, and iron oxide powders over 24 h, which led to the formation of nanocrystals with a size of nearly 20 nm. It has been found that the material exhibits a catalytic property for preparing carbon nanotubes. Liu et al.<sup>[24]</sup> used  $\text{MgO}/\text{Fe}_2\text{O}_3$  mixture for the synthesis of the Fe/MgO nanocomposite. To prepare MgO/Fe nanocomposites, the mixture was milled along with Mg powder for 24 h. The catalytic growth of carbon nanotubes and carbon-encapsulated Fe nanoparticles were conducted in a tube furnace. Methane ( $\text{CH}_4$ ) was used as the carbon source and the carbonization was performed at the temperature range of 700–900°C in Ar- $\text{CH}_4$  gas mixture.

To the best of our knowledge, all nanocomposite catalysts produced by previous investigators needed to process in two or three steps, while the most promising point in the current research is that nanocatalysts were produced in one milling step without needing to any further treatment. In the present work, we used the mixture of Al,  $\text{Fe}_2\text{O}_3$ , and graphite powders with different weight percents of graphite to synthesize C- $\text{Al}_2\text{O}_3$ -Fe composite particles by mechanical milling. The phase transformations during milling process were investigated. The chemical reaction involved here can be expressed as:  $2\text{Al} + \text{Fe}_2\text{O}_3 + \text{C} \rightarrow 2\text{Fe} + \text{Al}_2\text{O}_3 + \text{C}$ . After synthesizing mechano-nanocomposite particles, they were applied successfully as catalysts for CNTs production.

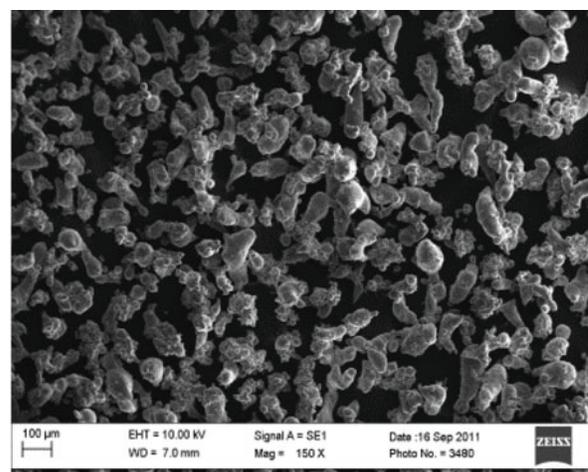
## EXPERIMENTAL

### Materials

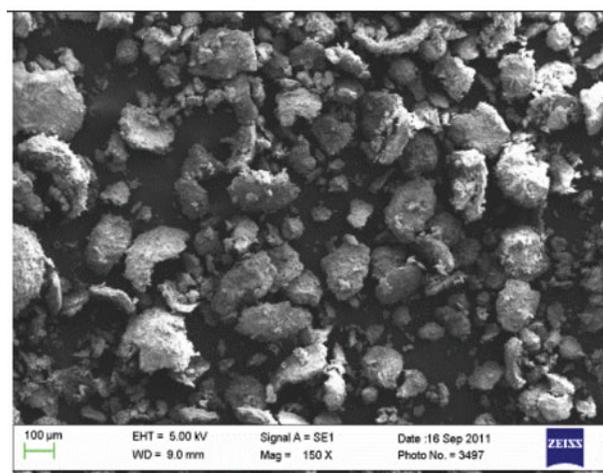
Commercially pure Al (purity more than 99%,  $<100 \mu\text{m}$ ),  $\text{Fe}_2\text{O}_3$  (purity more than 99%,  $<100 \mu\text{m}$ ), and graphite (purity of 99.9%,  $<200 \mu\text{m}$ ) powders all from Sigma-Aldrich Co. were used as raw materials in this study. SEM micrographs of the starting powders are shown in Figure 1.

### Catalyst Synthesis

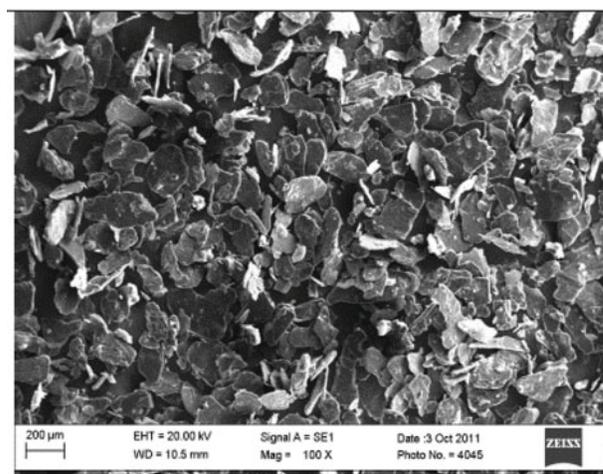
Several mixtures of iron oxide and aluminum powders along with different amounts of graphite powder were mechanically milled for different times using Planetary Mono Mill (Pulverisette6, Fritsch). The molar ratio of Al to  $\text{Fe}_2\text{O}_3$  was kept



a



b



c

FIG. 1. SEM images of initial materials: Al (a),  $\text{Fe}_2\text{O}_3$  (b), and graphite (c). (color figure available online).

TABLE 1

Different amounts of carbon in mixtures and related adiabatic temperatures

Carbon in a mixture, wt%	Adiabatic temperature, K
5	3130
10	2920
15	2740

constant 2:1 (according to thermite reaction stoichiometry:  $2\text{Al} + \text{Fe}_2\text{O}_3 = 2\text{Fe} + \text{Al}_2\text{O}_3$ ). Ball-milling was carried out at a rotation speed of 300 rpm under air atmosphere. Both vial ( $250 \text{ cm}^3$ ) and balls (10 mm in diameter) are made of tempered steels. The weight ratio of balls and starting powder was selected at 40. The vial was cooled by air during grinding. Milling times were varied from 0.5 to 72 h.

Since the ratio of the enthalpy (heat of reaction) to the heat capacity of the products ( $\Delta H/C$ ) at room temperature is more than 2000 K, which is required for the propagation of a self-sustaining reaction,<sup>[25]</sup> therefore, the adiabatic temperature and the heat released from exothermic reaction during milling were controlled by varying the percent of graphite (Table 1). This is because the formation of Fe and  $\text{Al}_2\text{O}_3$  from the reactants is a severely exothermic reaction.

### CNTs Synthesis

The synthesis of CNTs was carried out by a CVD method using nanocomposite powders obtained by ball milling ( $\text{Fe}/\text{Al}_2\text{O}_3/\text{C}$ ), mentioned in the detail previously, and the catalyst. The 0.15 g of catalyst was spread over a ceramic boat and placed in a tubular reactor. Propane ( $\text{C}_3\text{H}_8$ ) was used as the carbon source and the carbonization was performed at the temperature range of 625–850°C in  $\text{Ar}-\text{C}_3\text{H}_8$  mixture for 30 min. Propane was introduced into the gas stream at a flow rate of 30 mL/min diluted with 200 mL/min argon carrier. After reaction, the system was cooled down to room temperature and the products were characterized by transmission (TEM) and scanning electron microscopy (SEM), X-ray diffraction (XRD), and thermogravimetric analysis (TGA). The effect of growth temperature on the formation yield of CNTs was also examined by carrying out the propane decomposition reaction at different temperatures (i.e., 625, 700, and 850°C). The synthesized CNTs were cooled in Ar flow and the weight of deposited CNTs was measured. The yield of deposited carbon was calculated from the following equation:

$$\text{Yield} = ((W_2 - W_1)/W_1) \cdot 100\% \quad [1]$$

where  $W_1$  is the initial weight of the catalyst (milled products) and  $W_2$  is the weight of carbon deposited and catalyst.

### Instrumental Techniques

SEM observations were performed using a Zeiss EVO 50XVP at an accelerating voltage of 15 kV. Specimens for SEM were prepared by standard techniques, according to which a thin layer of powder was spread to the conductive adhesive tape. For better conductivity a thin layer of gold ( $\sim 10 \text{ nm}$ ) was deposited on the surface. The TEM analyses were carried out with a Tecnai 20 G2 model of FEI at an operating voltage of 200 kV. The obtained samples were dispersed ultrasonically in ethanol. A drop of the dispersed suspension was placed on a microgrid coated with thin layer of amorphous carbon and dried in air before fitting into the TEM apparatus. X-ray diffraction analysis performed by an ARL X'TRA advanced apparatus, using  $\text{Cu}-\text{K}\alpha$  radiation. Thermogravimetric analysis was performed using a NETZSCH STA 449 C at a heating rate of 10°C/min to warm the samples from room temperature up to 900°C in a mixture of argon (20 mL/min) and oxygen (10 mL/min) atmosphere.

## RESULTS AND DISCUSSIONS

### X-Ray Diffraction Examination

Figure 2 shows the XRD patterns of powder mixture containing  $\text{Al}-\text{Fe}_2\text{O}_3$ -5% graphite after different milling times. XRD patterns of milled powder up to 48 h identify a mixture of iron oxide ( $\text{Fe}_2\text{O}_3$ ), aluminum along with aluminum oxide, and iron, indicating that ball milling up to 48 h had gradual effect on as-received powder mixture. After 72 h ball milling, only peaks of iron and alumina (with a small peak of unreacted aluminum) are detected. It means that the reduction reaction, which is induced by ball milling, happened slowly. This result is similar to what proposed by other investigators. For example Schaffer and McCormick<sup>[21,26]</sup> studied the reduction of  $\text{CuO}$  by Ca using toluene as lubricant. The reduction of  $\text{CuO}$  proceeded gradually and completed in a day. When  $\text{CuO}$  was ball milled with

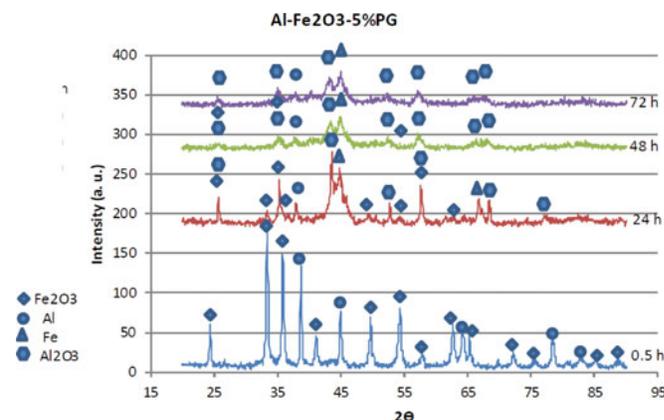


FIG. 2. XRD patterns of  $\text{Al}-\text{Fe}_2\text{O}_3$ -5%graphite ball milled for different times. (color figure available online).

reactive metals in the absence of any lubricant, a self-propagating combustion occurred after an incubation period.

It has been suggested that the value of adiabatic temperature ( $T_{ad}$ ) should be above 1800 K to yield self-propagating combustion reaction in a thermally ignited system.<sup>[27]</sup> However, in the current research and despite having  $T_{ad}$  greater than 1800K for selected mixture, no combustion reaction during ball milling was seen. The exact reason may be related to the role of graphite (because of its low density and high volume as well as high conductivity), which can suppress combustion happening. Arami et al.,<sup>[28]</sup> who studied mechanical induced reaction in Al-CuO system, also showed that although the reaction is highly exothermic and can be ignited at a high rate (i.e., self-propagation combustion reaction), the reaction occurred gradually and its rate was found to be depended on the mechanical alloying time. They attributed this phenomenon to the presence of excess aluminum in the system, which would suppress the self-propagation combustion reaction.

Since the adiabatic temperature of this mixture (Al-Fe<sub>2</sub>O<sub>3</sub>-5%graphite) according to Table 1 is higher than two other mixtures (containing 10% and 15% graphite) so one may conclude that the products are fabricated gradually as milling time increases. This is because the repeated welding and fracturing of powder particles increases the area of contact between the reactant powder particles due to a reduction in particle size and allow fresh surfaces to come into contact repeatedly. This allows the reaction to proceed without the necessity for diffusion through the product layer. As a consequence, reactions that normally require high temperatures will occur at lower temperatures during mechanical milling without any externally applied heat.<sup>[29]</sup> The lack of carbon peaks on XRD patterns is related to the lower intensity compared to the other materials. Perhaps the reason of this phenomenon can be attributed to the fact that the content of graphite in mixture is low as well as its low degree of crystallinity. Such a result has been shown in other researches. For example, Streletskii et al.<sup>[30]</sup> who studied mechanical treatment of aluminum with 10–30 wt% graphite in the high-energy vibration mills showed that as the dose of mechanical treatment increased, the graphite (002) peak widened, its maximum moved toward small angles (i.e., the graphite interlayer distance 002 increases), and, then, the line disappeared.

Figure 3 shows the XRD pattern of annealing products. This pattern is related to sample Al-Fe<sub>2</sub>O<sub>3</sub>-5%graphite milled for 48 h and then annealed under mixture of Ar (flow rate = 200 mL/min) and propane (flow rate = 30 mL/min) at 700°C for 30 min. XRD analysis reveals the formation of Al<sub>2</sub>O<sub>3</sub> and carbon phases. The XRD data suggest that the obtained carbon nanotubes which can observe in electron microscopy sections are built from well crystallized carbon ( $2\theta$  between 26° and 26.65°,  $d_{002} = 3.34$  Å).<sup>[31]</sup> As can be seen, the Fe peak is not obvious for synthesized products after annealing at 700°C, suggesting that the iron nanoparticles produced during ball milling have been used as catalysts for CNTs growth. This is why no significant amount of iron was appeared as free metallic particles.

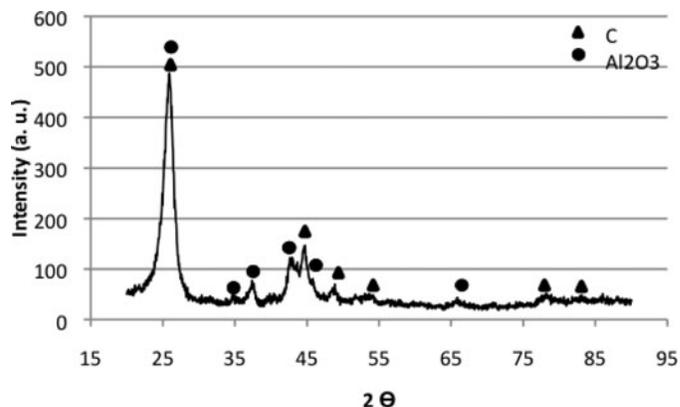


FIG. 3. XRD patterns of Al-Fe<sub>2</sub>O<sub>3</sub>-5%graphite ball milled for 48 h and annealed at 700°C under flow of Ar + C<sub>3</sub>H<sub>8</sub>.

### TGA

Figure 4 shows TGA curves of Al-Fe<sub>2</sub>O<sub>3</sub>-5%graphite samples milled for different times. It can be observed that there are two stepwise weight increases for all three samples. As would be expected, the material with a larger specific surface area and higher energy burns faster than the other materials. Furthermore, it is known that amorphous carbon is rather rapidly oxidized in air even at 350–400°C.<sup>[32,33]</sup> Therefore, first step can be assigned to burning out of amorphous carbon along with metallic un-reacted aluminum oxidation, and the second stage can be ascribed to oxidation of un-reacted aluminum and iron particles which resulted from the mechanochemical reaction (i.e.  $Al + Fe_2O_3 = 2Fe + Al_2O_3$ ). It can be seen that these materials start to be oxidized in oxidative atmosphere at a not significant rate up to temperature around 350°C and more significant after 350°C. So the first stage includes with two events, the first implies the weight loss because of amorphous carbon burning. The second event happens simultaneously with the first event and is related to the oxidation of un-reacted aluminum and leads to weight increase. Therefore, the first slight slope is due to balance between these two phenomena. After first stage in which amorphous carbon is completely burned out the only expected event can be

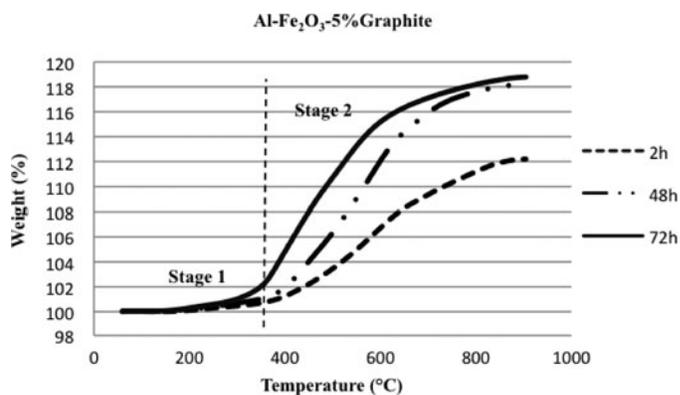


FIG. 4. Thermogravimetric analysis of Al-Fe<sub>2</sub>O<sub>3</sub>-5%graphite mixture, ball milled for different times.

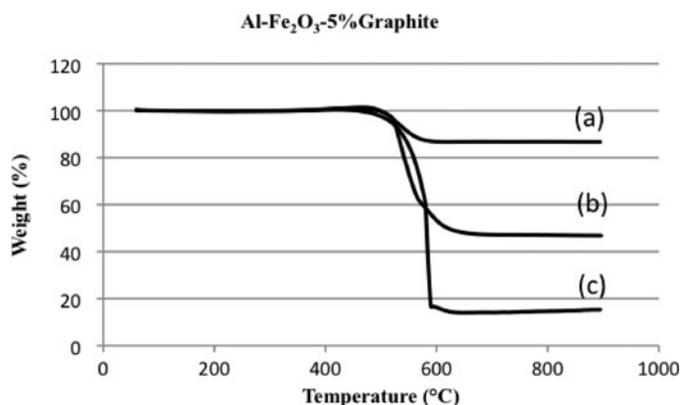


FIG. 5. Thermogravimetric analysis of Al-Fe<sub>2</sub>O<sub>3</sub>.5%graphite mixture ball milled for 48 h and annealed at 625°C (a), 700°C (b), and 850°C (c).

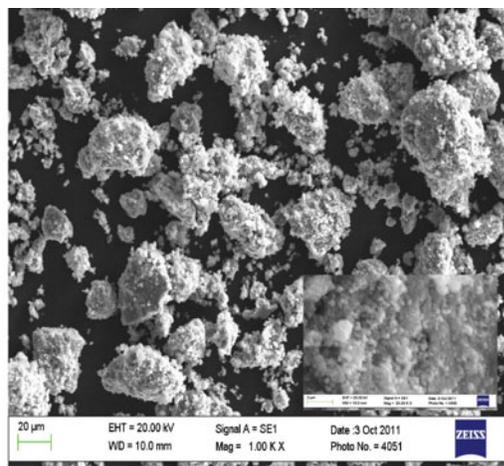
the oxidation of the metal particles. Consequently, it can be observed a higher oxidation rate for all samples in the second stage. All three samples show a similar oxidation behavior, but in the case of sample with 2h milling a little lower rate of weight increase is observed. It may be related to high oxidation resistance of aluminum because of its passive behavior in oxidation atmosphere. It means that after initial oxidation a dense layer of aluminum oxide covers the particles and suppresses the particle oxidation anymore which results in to lower weight increase in TGA. In the samples tested, the residual mass of mixture of alumina and iron oxide ranged from approximately 12 to ~19 wt% of the original sample weight. Furthermore, according to calculations, the percent of the mechanochemical reaction progress is about 50%, 80%, and 85% for the sample milled for 2, 48, and 72 h, respectively. Finally, based on the previous TGA data, It can be concluded that the reduction reaction of  $2Al + Fe_2O_3 = 2Fe + Al_2O_3$  happens gradually as milling time increases and it is in agreement with XRD results. Figure 5 shows the weight losses related to samples Al-Fe<sub>2</sub>O<sub>3</sub>.5%graphite ball milled for 48 h and then annealed at different temperatures for 30 min. All three samples have the same temperature in which oxidation just begins (about 510°C) while their maximum oxidation temperature is around 560°C. The oxidation temperature can be attributed to the carbon nanotubes because it is well known the CNTs have an oxidation temperature range between 500°C and 650°C.<sup>[32,34]</sup> Since the induced weight losses is related to CNTs oxidation one may calculate the weight percent of CNTs using TGA curve as mentioned in.<sup>[35]</sup> Therefore, for the sample having annealing temperature of 625°C, the amount of carbon nanotubes, determined from TGA curves, is about 13 wt%, while the samples having annealing temperature of 700°C and 850°C contains 53 wt% and 85 wt% carbon nanotubes, respectively. These results have a good agreement with SEM images.

### Microscopic Evaluations

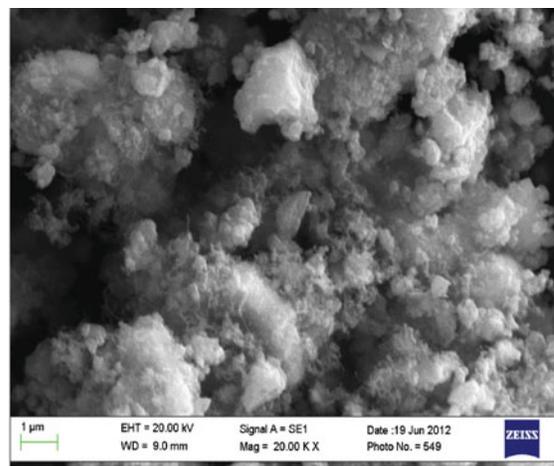
As it can be seen in Figure 1 both aluminum and iron oxide powders have irregular shapes with particle size below

100 μm. Graphite powders are plate-like shapes with average particles size of about 100 μm. Figure 6 shows the morphology of Al-Fe<sub>2</sub>O<sub>3</sub>.5%graphite composite powders milled at different times. As it can be seen, an increase in the milling time causes an increase in the probability of decreasing the particle size. The size of the produced particles decreases during milling and reaches from more than 100 μm to less than 5 μm (Al-Fe<sub>2</sub>O<sub>3</sub>.5%graphite 48 h). From the images inserted in Figure 6, milled powders appear relatively large agglomerations consisted of very fine particles. Smooth and dense surface morphology is observed, suggesting the occurrence of a kind of sintering. As a result, each of such large particles is a composite of ball milled graphite, Fe and Al<sub>2</sub>O<sub>3</sub> products. Figure 7 shows SEM micrographs of the ball-milled powders after annealing at different temperatures. According to SEM analysis the productivity of filaments grown on Al-Fe<sub>2</sub>O<sub>3</sub>.5%graphite catalyst at higher annealing temperatures (700°C and 850°C) is much greater than those grown at lower temperatures. It can be also observed that only some amounts of short, thin filaments synthesized at temperature 625°C and a few more at temperature 700°C but many long thin and thick filaments with various lengths up to several tens of microns grown at 850°C. There is an apparent change in the yield of carbon nanomaterials obtained (less than 10% for temperature 625°C and up to 320% for temperature 850°C) as well as their morphology. It is generally accepted that temperature affects the microstructure and yield of CNTs since catalytic activity and rate of decomposition of carbon on the catalytic particle from gas phase are significantly influenced by temperature. Growth of CNTs starts at temperatures in the neighborhood of 500°C at which there is enough mobility of the catalyst atoms to enable the diffusion of carbon through the particle and initiate the synthesis of nanotubes. The mobility of carbon in iron increases as temperature increases since the diffusion coefficient is highly dependent on temperature. This explains why the growth of CNTs is a thermally activated process. The rate of growth of CNTs increases with reaction temperature.<sup>[36]</sup> This can be attributed to the fact that the rate of decomposition of propane and the rate of diffusion of carbon in the metal particles increase with increasing temperature. In the case of filaments grown at lower temperature it has been reported,<sup>[37]</sup> that at the low temperature of deposition, carbon atoms form clusters which do not possess the required energy to arrange themselves into long-range ordered tubes, and it is in agreement with our case.

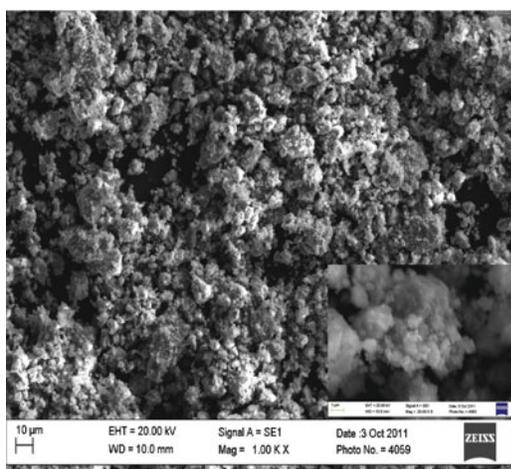
The chemical composition of the samples after annealing was also studied by energy dispersive X-ray spectroscopy (EDX). The typical EDX spectrum obtained from sample synthesized at 850°C is shown in the Figure 8. EDX analysis shows that the atomic percentages of carbon, oxygen, iron, and aluminum are 90.8, 7.5, 0.79, and 0.81, respectively. The signals of gold atoms are contributed to the gold-coated sample for better resolution of SEM images. Since the CNTs growth needs the iron nanoparticles as catalyst one may conclude that from EDX analysis the peaks of iron, aluminum, oxygen, and carbon must be



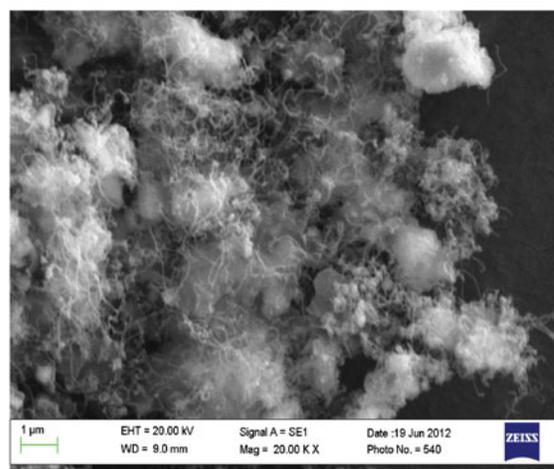
(a)



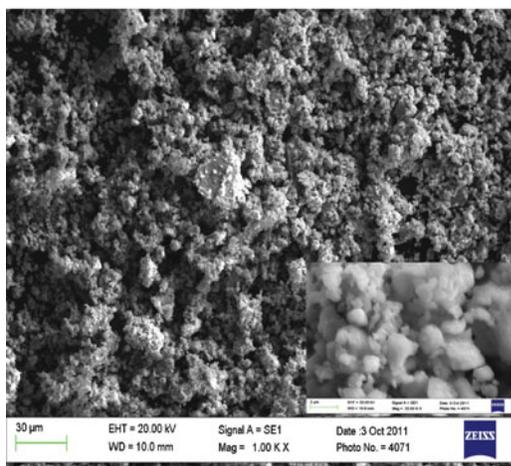
(a)



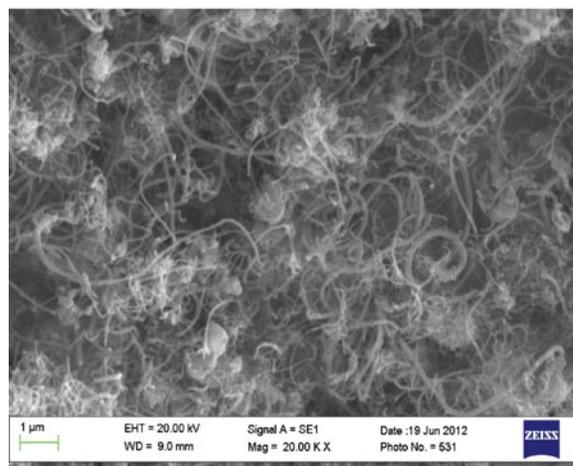
(b)



(b)



(c)



(c)

FIG. 6. SEM photographs of Al-Fe<sub>2</sub>O<sub>3</sub>-5%graphite composite powders obtained from ball milling at different times: (a) 2 h, (b) 24 h, and (c) 48 h. (color figure available online).

FIG. 7. SEM photographs of Al-Fe<sub>2</sub>O<sub>3</sub>-5%graphite composite powder that 48 h ball milled and then annealed at different temperatures for 30 min, 625°C (a), 700°C (b), and 850°C (c). (color figure available online).

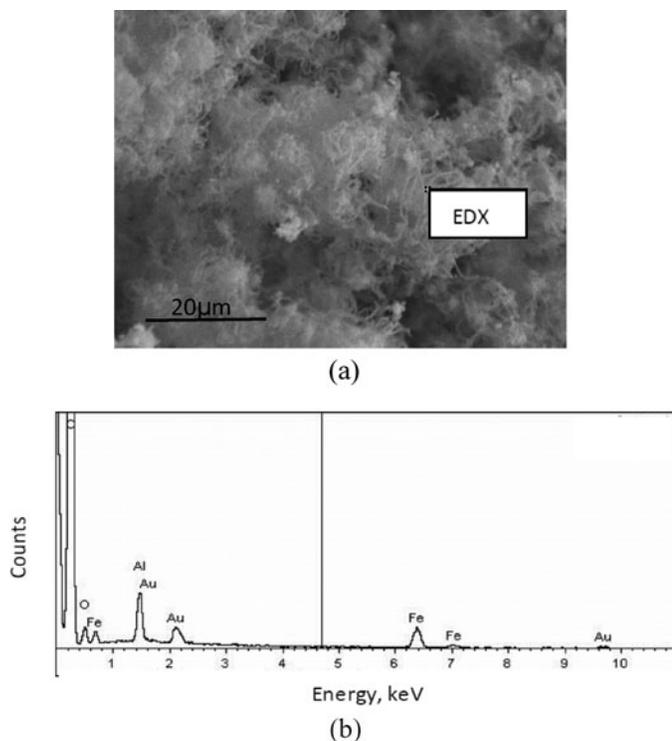


FIG. 8. SEM photographs of sample Al-Fe<sub>2</sub>O<sub>3</sub>.5%graphite which 48 h ball milled and then annealed at 850°C (a) and related EDX spectra (b).

corresponded to pure iron, aluminum oxide, and carbon nanotubes, respectively. Representative TEM and HRTEM images of the various Al-Fe<sub>2</sub>O<sub>3</sub>.5%graphite composite powders ball milled for different times and corresponding EDX spectrums are shown in Figure 9. With comparing the results of Figure 9, it can be concluded that with increasing milling time the size of product particles decreases. The second row in Figure 9 is shown many of these particles have a dimension less than 200 nm as well as each particle combines of many nano-sized components (dark spots in the light matrix). When comparing Figure 9, it is obvious that the number of nano-sized crystallites increases unlike their size with increasing milling time. It is seen that the single micron-sized particles observed in SEM images (Figure 6) are not an elementary one but are an aggregation of large number of smaller particles (less than 200 nm) agglomerated to each other. Figure 9 and the corresponding EDX demonstrate that the dark spots correspond to iron, aluminum, oxygen, and carbon. This dark spots are presented in the form of single nanoparticles with the sizes less than 20 nm. From Figure 9 it can be clearly seen that many of these nanoparticles are distributed and capsulated in some graphite shells. On the based on Figure 10, it can be concluded that a large number of dark spots (shown in Figures 9) are pure iron nanoparticles that led to the formation of CNTs.

The TEM images in Figure 10 show the morphology of the CNTs. The obtained carbon nanotubes appear as rather long and

curved multi-walled tubes that are usually bundled together. Also the diameters of these carbon nanotubes are relatively uniform throughout their length and in the range of 10–30 nm. Figure 10 shows a large number of tangled tubes, which form a massive web as well as some sharp dark particles. The higher magnification TEM image (Figure 10) shows that each of these sharp dark particles is the source of growing many CNTs. From Figure 10, it is obvious that the catalytic metal particles are located at the nanotubes tip and the EDX pattern derived from the particle at the tip of CNT shown in Figure 10 indicates that the composition is pure iron.

So, one can speculate the growth mechanism of carbon nanotubes is tip-growth using iron nanocatalysts. Consequently, it seems that sharp dark particles (e.g., see the EDX pattern in Figure 10) are composite powders including pure iron nanocatalysts, aluminum oxide, and ball-milled graphite. These results demonstrate that the mechanochemical method can be a promising process for the production of catalysts for the catalytic growth of carbon nanotubes. It might be explained by the iron nanoparticles resulted from mechanochemical reaction in a porous structure of the support which makes it permeable to the propane molecules so that carbon feedstock reaches the catalyst at a high rate, as mentioned in previous work.<sup>[4]</sup> It is believed that the graphite, which is ball milled along with Al and Fe<sub>2</sub>O<sub>3</sub>, plays important role to produce iron nanoparticles. Firstly, the use of graphite acts as an additive (diluent) and either delays or completely suppresses the combustion event (as it has been shown in XRD and TGA section before). The graphite also inhibits interparticle welding during collisions, slowing down the reaction rate as well as decreasing the particle size.<sup>[38,39]</sup> It is worth noting that to achieve a nanocrystalline metal combustion reaction must be postponed. This is because the result of combustion may be partially melting and subsequent solidification which leads to the formation of a coarse-grained structure. Second, ball milled graphite has a porous structure, which increases the permeability of mechanochemical-derived particles, and so propane reaches to iron nanocatalysts very easily. Apart from graphite, since the density of the Fe<sub>2</sub>O<sub>3</sub> phase (5.24 g/cm<sup>3</sup>) is lower than that of the Fe metallic phase (7.87 g/cm<sup>3</sup>), it is conceivable that a reduction in volume occurs with the nucleation and growth of Fe particles. As a result, a large number of pores are produced around newly formed Fe particles. Finally, according to tip-growth mechanism,<sup>[40]</sup> the catalytic nanoparticles at high temperature absorb carbon atoms from the propane to form a metal-carbon solid state solution. When this solution becomes supersaturated, carbon precipitates at the surface of the particle in its stable form and this leads to the formation of a carbon tube structure. The metal-support interactions are found to play a determinant role for the growth mechanism.<sup>[40,41]</sup> Weak interactions yield tip-growth mode whereas strong interactions lead to base growth. In our case we believe that the iron nanoparticles have a weak interaction with support, which leads to the formation of CNTs through tip-growth mechanism.

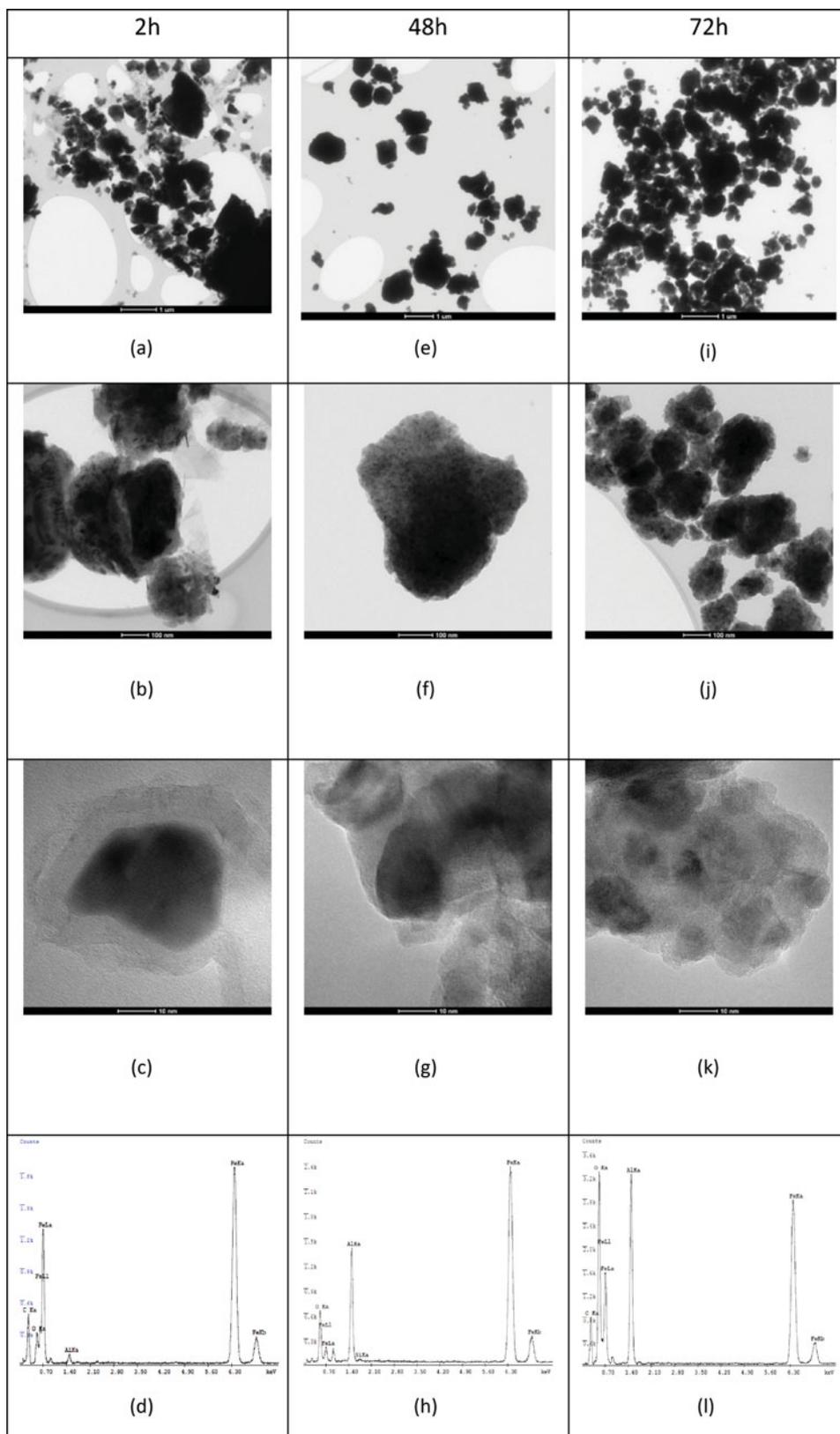
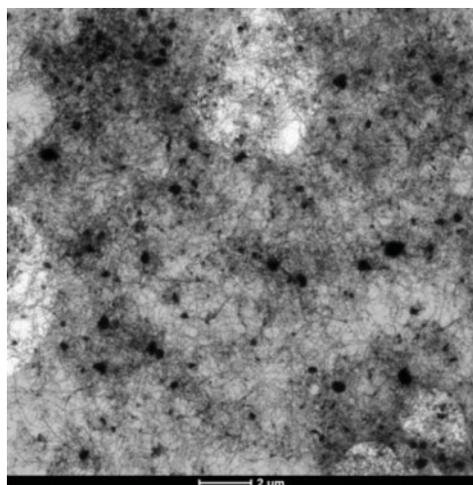
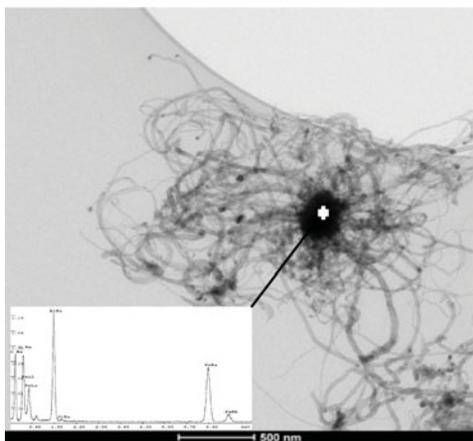


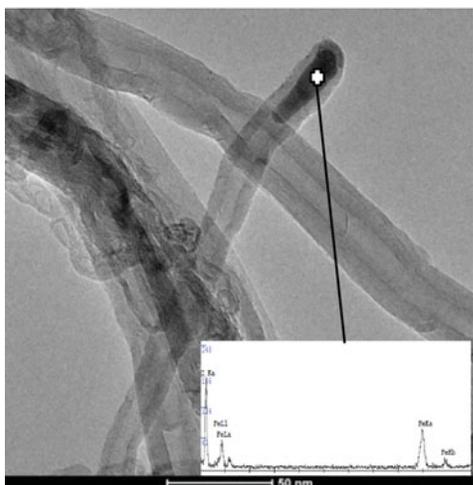
FIG. 9. TEM images of Al-Fe<sub>2</sub>O<sub>3</sub>.5%graphite composite powders ball milled for different times (a–c) 2 h, (e–g) 48 h, and (i–k) 72 h, and corresponding EDX spectrums of dark particles that go to (c, g, k). (color figure available online).



(a)



(b)



(c)

FIG. 10. TEM images of Al-Fe<sub>2</sub>O<sub>3</sub>/5%graphite composite powders ball milled for 48 h and annealed in 850°C in different magnification and related EDX patterns. (color figure available online).

## CONCLUSION

The aim of the research was to use reactive milling to fabricate the nanocomposite precursors as catalyst for the catalytic growth of carbon nanostructures. For this purpose several mixtures of iron oxide and aluminum powders along with different amounts of graphite powders were mechanically milled for different times. A gradual mechanochemical reaction between reactants was observed, which led to the formation nanocomposites containing aluminum oxide, graphite, and iron nanoparticles. These nanocomposites were also used successfully for catalytic growth of carbon nanotubes. Carbon nanotubes were synthesized through a tip-growth mechanism with CVD process. It was found that the yield of carbon nanotubes formation was dependent on the annealing temperature and increased as temperature increased.

## REFERENCES

- Zhang, Q.; Huang, J.Q.; Zhao, M.Q.; Qian, W.Z.; Wei, F. *ChemSusChem* **2011**, *4*, 864.
- Altay, M.C.; Eroglu, S. *Diamond Relat. Mater.* **2013**, *31*, 19.
- Paradise, M.; Goswami, T. *Mater. Des.* **2007**, *28*, 1477.
- Dupuis, A.C. *Prog. Mater. Sci.* **2005**, *50*, 929.
- Chiang, W.H.; Sankaran, R.M. *Diamond Relat. Mater.* **2009**, *18*, 946.
- Luisetto, I.; Pepe, F.; Bemporad, E. *J. Nanopart. Res.* **2008**, *10*, 59.
- Narkiewicz, U.; Podsiadly, M.; Arabczyk, W.; Wóznia, M.J.; Kurzydowski, K.J. *Mater. Sci. Eng. C.* **2007**, *27*, 1273.
- Hernadi, K.; Fonseca, A.; Nagy, J.B.; Bernauer, D.; Fudala, A.; Lucas, A.A. *Zeolites* **1996**, *17*, 416.
- Park, H.; Afzali, A.; Han, S.J.; Tulevski, G.S.; Franklin, A.D.; Tersoff, J.; Hannon, J.B.; Haensch, W. *Nat. Nanotechnol.* **2012**, *7*, 787.
- Sengupta, J.; Jacob, C. *J. Nanopart. Res.* **2010**, *12*, 457.
- Dündar-Tekkaya, E.; Karatepe, N. *WASET* **2011**, *55*, 225.
- Flahaut, E.; Govindaraj, A.; Peigney, A.; Rousset, A.; Rao, C.N. R. *Chem. Phys. Lett.* **1999**, *300*, 236.
- Melezhik, A.V.; Sementsov, Yu.I.; Yanchenko, V.V. *Russ. J. Appl. Chem.* **2005**, *78*, 924.
- Tsuzuki, T.; McCormick, P.G. *J. Mater. Sci.* **2004**, 5143.
- Ghasemi, B.; Najafzadeh-Khoei, A.A. *Eng. Technol.* **2012**, *61*, 511.
- Kim, J.W.; Chung, H.S.; Lee, S.H.; Oh, K.H.; Shim, J.H.; Cho, Y.W.; *Intermetallics*. **2007**, *15*, 206.
- Povstugar, I.V.; Streletskii, A.N.; Permenov, D.G.; Kolbanov, I.V.; Mudretsova, S.N. *J. Alloys Compd.* **2009**, *483*, 298.
- Anvari, S.Z.; Karimzadeh, F.; Enayati, M.H. *J. Alloys Compd.* **2009**, *477*, 177.
- Ding, J.; Miao, W.F.; McCormick, P.G.; Street, R. *Appl. Phys. Lett.* **1995**, *67*, 3804.
- Melezhik, A.V.; Yanchenko, V.V.; Sementsov, Y.I. *Natl. Security Sci. A.* **2007**, 529.
- Schaffer, G.B.; McCormick, P.G. *Appl. Phys. Lett.* **1989**, *55*, 45.
- Grigorieva, T.F.; Barinova, A.P.; Lyakhov, N.Z. *J. Nanopart. Res.* **2003**, *5*, 439.
- Guo, X.; Qi, J.; Sakurai, K. *Scripta Mater.* **2003**, *48*, 1185.
- Liu, B.H.; Ding, J.; Dong, Z.L.; Zhong, Z.Y.; Lin, J.Y.; White, T. *Solid State Phenom.* **2006**, *111*, 183.
- Munir, Z.A.; Anselmi-Tamburini, U. *Mater. Sci. Rep.* **1989**, *3*, 277.
- Schaffer, G.B.; McCormick, P.G. *J. Mater. Sci. Lett.* **1990**, *9*, 1014.
- Li, J.; Li, F.; Hu, K. *J. Mater. Process. Technol.* **2004**, *147*, 236.

28. Arami, H.; Simchi, A.; Seyed-Reihani, S.M. *J. Alloys Compd.* **2008**, *465*, 151.
29. Suryanarayana, C. *Prog. Mater. Sci.* **2001**, *46*, 1.
30. Streletskii, A.N.; Kolbanev, I.V.; Borunova, A.B.; Butyagin, P.Y. U. *J. Mater. Sci.* **2004**, *39*, 5175.
31. Cao, A.; Xu, C.; Liang, J.; Wu, D.; Wei, B. *Chem. Phys. Lett.* **2001**, *344*, 13.
32. Dervishi, E.; Li, Z.; Biris, A.R.; Lupu, D.; Trigwell, S.; Biris, A.S. *Chem. Mater.* **2007**, *19*, 179.
33. Liu, J.; Harris, A.T.; *Chem. Eng. Sci.* **2009**, *64*, 1511.
34. Ratkovic, S.; Kiss, E.; Boskovic, G. *Chem. Ind. Chem. Eng. Q.* **2009**, *4*, 263.
35. Harutyunyan, R.A.; Pradhan, B.K.; Chang, J.; Chen, G.; Eklund, P.C.; *J. Phys. Chem. B* **2002**, *106*, 8671.
36. Alexiadis, V.I.; Verykiosa, X.E. *Mater. Chem. Phys.* **2009**, *117*, 528.
37. Zhao, N.Q.; He, C.N.; Du, X.W.; Shi, C.S.; Li, J.J.; Cui, L. *Carbon*. **2006**, *44*, 1859.
38. Froyen, L.; Delacy, L.; Niu, X.P.; LeBrun, P.; Peytour, C. *JOM* **1995**, *47*, 16.
39. Morris, D.G.; Morris, M.A. *Mater. Sci. Eng. A* **1990**, *125*, 97.
40. Baker, R.T. K. *Carbon* **1989**, *27*, 315.
41. Cassel, A.M.; Raymakers, A.; Kong, J.; Dai, H. *J. Phys. Chem. B* **1999**, *103*, 6484.